Silicon (2022) 14:2635–2646
https://doi.org/10.1007/s12633-021-01048-w

ORIGINAL PAPER

Characterization of Fly Ash Sources in the Synthesis of Geopolymer

Thulasirajan Krishnan[1] · Revathi Purushothaman[1]

Received: 6 November 2020 / Accepted: 3 March 2021 / Published online: 15 March 2021

Abstract
Fly ash (FA) based geopolymers are affected by the reactive nature of FA, concentration and quantity of alkali activators and the curing conditions. However, for the geopolymer production, researchers are still focusing on the concentration and quantity of alkali activators and the curing conditions. In the present study, FAs from two distinct thermal power plants and their activated geopolymer paste were investigated under physical, chemical, spectroscopic, mineralogical and microstructural characterizations. Based on the characterizations, the suitability of FAs for the geopolymer production was determined and validated by the compressive strength of geopolymer concrete. Additionally, the effect of critical parameters such as sodium hydroxide (NaOH) molarity, alkaline to FA ratio, curing time and curing temperature were studied. From the results, it is inferred that the FA's potential reactivity is to be identified through its characterization techniques before the synthesis of geopolymers. The quantity of vitreous silica (Si) and alumina (Al) contents in the FA significantly affects the geopolymerisation process. In order to choose the right source of FA, it is required to characterize the FA and its activated geopolymer paste. Thereby, the wide variation of the geopolymer synthesis parameters that leads to undesirable production cost and hazardous work environment can be avoided.

Keywords Geopolymer · Fly ash · Alkali activation · Microstructure · Vitreous content · Compressive strength

1 Introduction

Majority of power stations uses coal fuel for the generation of electricity. An enormous amount of FA is generated by incineration of coal. In India, the FA generated during the year 2018–2019 was roughly 217.04 million tons. Only 168.40 million tons was used in diverse applications [1]. Although FA's utilization acquired a tremendous growth and new status of a beneficial and saleable commodity in different fields, the remaining 48.64 million tons of FA remains idle covering a large area of valuable lands and prompts environmental pollution. Scientists are thus attempting to build new technologies to ensure the appropriate use of FA. One such emerging technology is the use of FA in geopolymers. Geopolymers were formed by alkali activation of partly or entirely vitreous alumina (Al) and silica (Si) minerals while cured at mild temperatures. Thereby, the vitreous three-dimensional solid cementitious matrix, namely sodium Al-Si hydrate (N-A-S-H) gel was formed [2, 3].

✉ Thulasirajan Krishnan
kthulasirajan@gmail.com

[1] Department of Civil Engineering, Pondicherry Engineering College, Pillaichavadi, Puducherry 605-014, India

The reactive nature of FA, the concentration and quantity of alkali activators, and the curing conditions impact the properties of FA-based geopolymers. However, for the synthesis of FA-based geopolymers, researchers focused only on the parameters such as the ratio of alkaline to FA (0.45 to 0.8), NaOH molarity (4.5 M to 16.5 M), curing time (6 h to 48 h) and curing temperature (60 °C to 120 °C) [4–11]. The compressive strength property acted as an indicator for the optimization of these parameters. In reality, the lack of sufficient knowledge of FA reactivity and extreme variation of these parameters would subsequently contribute to a rise in production cost, time and hazardous work environment [12–18]. Therefore, before the production of geopolymer concrete, it is obligatory to characterize the FA by examination of its fineness, quality and quantity of vitreous Al-Si systems using different characterization (analytical and instrumental) techniques. Hence, the understanding of its reactive nature can be acquired for its effective utilization in geopolymer concrete. The studies on characterizations of FAs related to geopolymer synthesis by different characterization techniques are presented in Table 1.

The physical characterization through the particle size distribution involved a crucial role in the manufacture of geopolymer. The fineness of FA enhanced the reactivity of FA [19, 25, 26]. The SiO_2 and Al_2O_3 were the main

Table 1 Literature review on characterization of FAs

Location	Number of FA Sources	Physical	Chemical	Spectroscopic		Minera-logical	Micro-structural	Reference
		Particle size	XRF	FITR	NMR	XRD	SEM	
Australia	3	*	*			*		[19]
Australia and Mongolia	5		*				*	[20]
Australia	3		*			*		[21]
Europe	7			*	*			[22]
Serbia	3				*	*	*	[23]
Poland	1	*	*	*		*	*	[24, 25]
Australia	5	*	*			*		[26]
India	1			*		*		[27]

Note : SEM- Scanning Electron Microscopy, XRF- X-Ray Fluorescence, XRD- X-ray Diffraction, FITR- Fourier Transform Infrared, NMR- Nuclear Magnetic Resonance

constituents in the three-dimensional structural frame of geopolymer. The chemical characterization by XRF analysis involved in the identification of the SiO_2 and Al_2O_3 constituents in FA. Moreover, the CaO percentage aided in the classification of FA as Class C or Class F [19–21, 23, 25]. However, the relative percentages of vitreous SiO_2 and Al_2O_3 constituents present in the FA were responsible for the N-A-S-H gel formation. Identification of the vitreous Al-Si constituents by chemical attack rendered in the development of strength enhanced geopolymers [21, 23, 26]. The formation of geopolymer products with structural reorganization was analyzed by FTIR spectra. FTIR was a relatively faster screening method for detection of various forms of Al-Si species [22, 24, 27]. NMR spectra analysis the identification of different Al-Si species and their bonds with the number of Al cross-linked with Si units which were responsible for the high strength of geopolymer [22]. The reactivity of Al-Si contents was influenced by the non-vitreous mullite [28]. The XRD pattern analysis the presence of crystalline phases and their leaching by the alkaline solution were indicated by reduction in corresponding peak intensities of geopolymer. Moreover, the undetected crystalline phases in the XRD ranges were the sign of the presence of vitreous Al-Si components [19, 21, 23–27]. The different type of FA exhibited heterogeneous behaviour when activated with alkaline solution. The morphology of the FA was assessed by analysis of SEM images which influence the workability and the surface texture of geopolymer [20, 23, 24, 29].

Strength of the geopolymer dependent on the finer particle size, vitreous contents (Al & Si), location of the peak crystalline phase and high fractions of aluminium rich structural units [19, 23, 30]. Hence, a better understanding of FA reactivity through characterization of the FA plays an integral part in geopolymer production.

Among, the common alumino-silicates sources, such as fly ash, metakaolin and ground-granulated blast-furnace slag, fly ash was considered in the present study. The reasons are the low cost of purchase and production, global coal reserves and prevent the unnecessary mass dumping in landfills and underwater bodies, thereby eliminate the potential risk to the environment and human [31].

From the review of literature, it is inferred that different techniques such as particle size distribution, XRF, FTIR, NMR, XRD and SEM are available for the characterization of FAs. As tabulated in Table 1, researchers applied one or more of these techniques to characterize different FA samples in different locations. However, proper knowledge on all the characterization techniques (refer Table 1) are required to understand the reactive nature of FA and its activated geopolymer pastes. Thereby the FA can be effectively utilized in the geopolymer concrete production by reducing the cost, time and hazardous work environment. To the author's knowledge, characterization of FA and their activated geopolymer pastes by all the techniques is not performed in a single framework. Moreover, extension of study to assess the compressive strength of geopolymer concrete produced by the characterized FA and the influence of standard parameters (alkaline to FA ratio, NaOH molarity, curing time and curing temperature) are not reported.

Hence, this paper aims to characterize the FAs from two different sources and their influence on the compressive strength of the geopolymer concrete. Different characterization techniques such as particle size distribution, XRF, FTIR, NMR, XRD and SEM were performed in a single framework for the FA and its activated geopolymer paste. The need for this characterization of FAs was demonstrated by assessment of the geopolymer concrete's compressive strength and the influence of variation of standard parameters such as alkaline to FA ratio, NaOH molarity, curing time and curing temperature was also studied.

2 Experimental Investigation

2.1 Materials

FAs procured from coal combustion processes of two different thermal power plant sources, namely, Ennore Thermal Power Plant situated in Tamil Nadu, India and Udupi Thermal Power Plant situated in Karnataka, India were considered for the current study. The capacities of Ennore and Udupi Power Plants were 450 MV and 1200 MV, respectively. Bituminous coal with an ash content of 34 % was used as fuel in Ennore Thermal Power Plant. Anthracite coal with an ash content of 12 % was used as fuel in Udupi Thermal Power Plant. The Ennore FA and Udupi FA are denoted as EFA and UFA respectively. A blend of NaOH and sodium silicate (Na_2SiO_3) was used for the activation of FA. The composition of Na_2SiO_3 was $Na_2O = 15.2$ %, $SiO_2 = 29.7$ % and $H_2O = 55.1$ % with a density of 1530 kg/m^3. The NaOH solution was prepared from flakes of 98 % purity. Since the addition of NaOH flakes and tap water releases a significant amount of heat, the molarity of NaOH solution was prepared prior to a day of use [5, 12, 14]. The molarity of NaOH considered for the characterization of activated FAs was 10 M [15].

2.2 Geopolymer Paste

Geopolymer paste was made by blending the alkaline solution and FA in the ratio of 0.65. The Na_2SiO_3 and NaOH ratio used was 2.5:1. The temperature maintained in the hot air oven was 60 °C and for 6 h. The geopolymer pastes produced from Ennore FA and Udupi FA are labelled as 'EGP' and 'UGP' respectively.

2.3 Geopolymer Concrete

Geopolymer concrete was produced to validate the suitability of FAs sources. The geopolymer concretes produced by Ennore FA, and Udupi FA are designated as EGC and UGC respectively. The FA, Na_2SiO_3, NaOH, river sand, crushed granite coarse aggregate and sulphonated naphthalene superplastizers were used the ingredients. The coarse aggregate and river sand were passing 10 mm and 4.75 mm size sieve respectively. The specific gravity of coarse aggregate and river sand were 2.73 and 2.68 respectively. The water absorption of coarse aggregate and river sand were 0.93 % and 1 % respectively. The amount of ingredients is presented in Table 2. For the manufacture of geopolymer concrete, conventional mixing method was adopted. Compaction was performed by using standard table vibrator. The specimens were mounted in the oven and cured for a specified time (6 h or 24 h) maintained a high temperature (60 °C or 90 °C). Then the specimens allowed to cool in the ambient temperature until testing (24 h). An average of six specimens was considered for the determination of compressive strength.

Table 2 Quantities of ingredients

Ingredients	Quantities (kg/m^3)
Coarse aggregate	1201.2
River sand	646.8
FA	380.7
Na_2SiO_3	122.4
NaOH	48.95
Superplasticizer	7.614

2.4 Methods

2.4.1 Physical Characterization

The laser particle size analyzer Mastersizer, Malvern Instruments Ltd., was used to determine the distribution of the particle of FAs. The dispersant agent used was ethylene glycol and tested at 24.9 °C in a measurement position of 0.85 mm. The count rates of EFA and UFA were 192.3 kcps and 520.6 kcps respectively.

2.4.2 Chemical Characterization

The chemical compositions of FAs were analyzed by X-Ray Fluorescence (XRF) using the X-ray analytical microscope XGT-2700, HORIBA, Japan with 60 s live time, 100 μm XGT diameter, 1 mA current and 50 kV X-ray tube voltage.

The percentage of reaction products present in the hardened geopolymer paste was determined by selective chemical attack. The hardened geopolymer paste was finely powered and targeted with 35 % concentrated hydrochloric acid (HCl) in the ratio of 1:20. The HCl was supplied by Emplura Company. The experimental procedure consisted of mixing 1 g of accurately weighed geopolymer (powder) to a 250 ml of HCl solution and stirred for three hours at a regular interval of 5 min duration. A filter paper of pore size between 15 μm and 20 μm fitted to filtration assembly and the suction pump was used for the mixture's filtration. The filtered mixture was then rinsed with deionized water to achieve neutral pH, dried for one hour in the oven at 100 °C, and calcined in the muffle furnace to 800 °C. The weight loss in this process was deduced to determine the dissolved phase percentage [32, 33].

2.4.3 Spectroscopic Characterization

The spectroscopic characterizations of FAs and the hardened geopolymer pastes were carried out using Fourier Transform Infrared (FTIR) Spectroscopy and ^{29}Si MAS solid-state Nuclear Magnetic Resonance (NMR) Spectroscopy.

FTIR analysis was conducted using ThermoFisherTM NicoletTM iSTM 5 FTIR spectrometer. Potassium bromide (KBr) pellets method was followed to prepare the specimens with 1 mg of sample in 200 mg of KBr. The specimens were scanned in the range of 500 cm^{-1} to 4000 cm^{-1}.

^{29}Si MAS solid-state NMR spectroscopy analysis was performed using Avance 400 MHz Bruker analyzer. The resonance frequency of 79 MHz with a 7 kHz spinning rate was used in the present study. The chemical shift reference used was tetramethylsilane and measurements were recorded at ambient temperature. The probe diameter used was 4 mm. The spectra were recorded at 25 μs with a time delay of 10 s.

2.4.4 Mineralogical Characterization

The mineralogical characterization was conducted by X-ray Diffraction (XRD) analysis of the FA and the hardened geopolymer paste. The XRD pattern was measured by using panalytical X'Pert pro X-ray diffractometer with CuKα1,2 radiation at 30 mA and 40 kV. The diffraction pattern was recorded within 10.02° − 80.92° 2θ range, by 0.05° 2θ step size, divergence slit of 0.4785° and time per step of 10.16 s.

2.4.5 Microstructure Characterization

The microstructure of the FAs and the hardened geopolymer pastes (crushed to powder) was examined by JEOL JSM 6610LV Scanning Electron Microscopy. The platinum-coated samples were placed on stubs with adhesive carbon pads before the capture of images. The images were captured in the range of 5 μm to 50 μm with an accelerating voltage of 10 kV.

2.4.6 Compressive Strength

The compressive strength of geopolymer concrete was tested by AIMIL compressive testing machine of 3000 kN capacity. The cube specimens were positioned in the compressive testing machine, and the compressive load was applied at 14 MPa per minute.

3 Experimental Results and Discussion

3.1 Physical Characterization

The percentage volume of EFA and UFA is shown in Fig. 1. The fraction of particles less than 10 %, 50 % and 90 % of the total volume are denoted as D10, D50 and D90 respectively. The UFA's particle sizes were ranged from 1 μm to 70 μm with D10 = 11.37 μm, D50 = 31.05 μm and D90 = 57.9 μm. The EFA's particle sizes were ranged from 2 μm to 120 μm with D10 = 24.92 μm, D50 = 63.62 μm and D90 = 114.6 μm. It is seen that the UFA particle size is comparatively finer than that of EFA. The smaller size of FA particles possesses high vitreous content [34], which eases the faster dissolution in alkaline solution than the EFA.

3.2 Chemical Characterization

The chemical compositions of the FAs obtained from XRF analysis are presented in Table 3. It is noted that the percentages of calcium present in EFA and UFA were 0.97 % and 5.14 % respectively. According to the standards of ASTM C 618 [35], the CaO percentages were less than 10 %, and therefore both FAs were categorized as Class F of low calcium content. Further, the total percentage of SiO_2 and Al_2O_3 components present in EFA and UFA were found to be 83.71 % and 72.18 % respectively. The calculated ratios of SiO_2 to Al_2O_3 present in EFA and UFA were 4.79 and 3.65 respectively. From these results, it is observed that the Al-Si constituents are rich in EFA when compared to those of UFA. However, the amount of reactive Al and Si constituents for geopolymerisation is unrecognized.

The amount of reactive product formed during the alkaline activation was determined by selective chemical attack. The reactive product soluble in chemical attack resulted in transparent crystals, which is attributed to N-A-S-H gel [36]. The percentages of insoluble residues present in EGP and UGP were 71.72 % and 51.24 % respectively. Thereby, the percentages of N-A-S-H gel (transparent crystals) formed in EGP and UGP were 28.28 % and 48.76 % respectively. As compared to EFA, the percentage of the reactive product is higher in UFA due to the high amount of reactive Al and Si constituents. Moreover, from the previous studies, it is inferred that the performance of geopolymer would be useful, if the degree of reactivity was greater or around 50 % [36, 37]. The quantity of reactive products formed in activated geopolymer paste is not equal to the quantity of Al and Si constituents found in the FA sources. Therefore, in addition to the chemical composition analysis, NMR and XRD characterization techniques are required to select FA's right source.

3.3 Spectroscopic Characterization

3.3.1 FTIR Analysis

The comparison of FTIR spectrums of EFA and UFA along with its geopolymer are shown in Figs. 2 and 3 respectively. FTIR spectrum of EFA shows distinct bands/signals at 3445.04 cm^{-1}, 1614.45 cm^{-1}, 1093.84 cm^{-1}, 796.33 cm^{-1} and 694.41 cm^{-1}. FTIR spectrum of UFA also shows distinct bands at 3444.54 cm^{-1}, 1633.56 cm^{-1}, 1044.07 cm^{-1} and 775.84 cm^{-1}. EFA and UFA spectra shows wide and intense

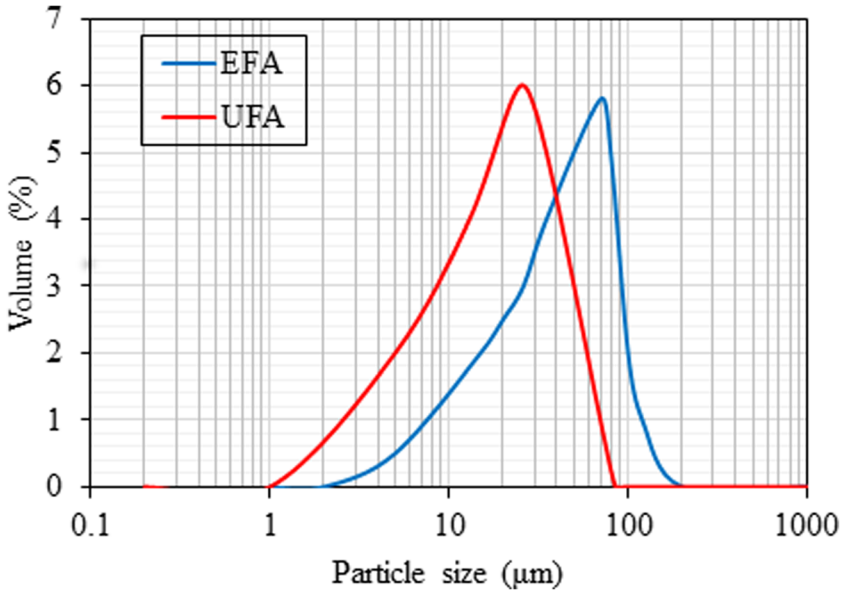

Fig. 1 Distribution of particle size in FAs

bands at 1093.84 cm^{-1} and 1044.07 cm^{-1} respectively, which is linked to the asymmetric stretching vibrations with T-O bond (T = Si, Al). The narrow bands at 796.33 cm^{-1} (double band) and 694.41 cm^{-1} revealed crystalline quartz minerals in EFA.

The occurrence of geopolymerization reaction is justified by the formation of the bonds between Al and Si. The band at 1093.84 cm^{-1} of EFA shifted to 1021.42 cm^{-1} in the corresponding EGP. Similarly, the band at 1044.07 cm^{-1} of UFA shifted to 1018.09 cm^{-1} in the corresponding UGP. Thus, the shift of band to lower values indicates the intrusion of Al in the Si-O-Si bond and attributes to asymmetric stretching vibrations. Further, the magnitude of variation during this intrusion process was controlled by the FA's reaction time [3]. Thus from this spectrum shifts, it is revealed that EFA requires more reaction time than that of UFA. Moreover, the signals appeared around 1025 cm^{-1} − 1006 cm^{-1} is attributed to the N-A-S-H gel [38].

Table 3 Chemical composition of FAs

Constituents	EFA (%)	UFA (%)
SiO_2	69.27	56.68
Al_2O_3	14.44	15.50
Fe_2O_3	1.84	4.98
CaO	0.97	5.14
Na_2O	7.49	8.83
TiO_2	1.33	1.49
MnO_2	0.04	0.06
SO_3	0.42	1.18
MgO	2.07	4.1
K_2O	0.73	1.03

The FTIR spectra of EGP and UGP show a distinct formation of a new band around 1448 cm^{-1}, which represents the presence of sodium carbonate. It may be developed by the carbonation of unreacted Na_2SiO_3 and/or NaOH. Substantial broad bands around 3450 cm^{-1} and 1650 cm^{-1} to 1600 cm^{-1} indicates the stretching and bending of O-H respectively. This is because of the weakly bound extra water molecules may be connected to the surface or trapped into the geopolymer cavities. When compared to UGP, the absorption of water molecules by EGP is more pronounced with wider bands. The activation of EFA with alkaline solution shifts the bands from 796.86 cm^{-1} to 796.33 cm^{-1} and 694.41 cm^{-1} to 693.63 cm^{-1}. These marginal band shifts justify the presence of crystalline quartz in EFA, which barely affected by the activation process. However, the signal appeared at 775.84 cm^{-1} of UFA disappeared in UGP spectrum due to the presence of vitreous quartz minerals. Further, the absence of structural information related to the new signal appeared at 694.55 cm^{-1} may be categorized as vitreous or crystalline quartz [2, 39, 40].

3.3.2 NMR Spectra

The configuration and structural sorting of vitreous Al-Si systems are described by the NMR spectra [41, 42]. The Q^n (mAl) (m, n = 0 to 4) units are the traditional notation used to describe the Al-Si system with *n* denotes the Si centre coordination number and *m* denotes the number of Al all-round the Si with bridged oxygen bonds. The Al-Si systems were represented by Q^4 specifying the three dimensional cross link sites [43]. Figure 4 shows the ^{29}Si MAS NMR spectra of EFA and UFA along with their activated geopolymer pastes.

It is seen that the peak signals occurs at a chemical shift of -110.25 ppm and − 105.85 ppm in EFA and UFA respectively.

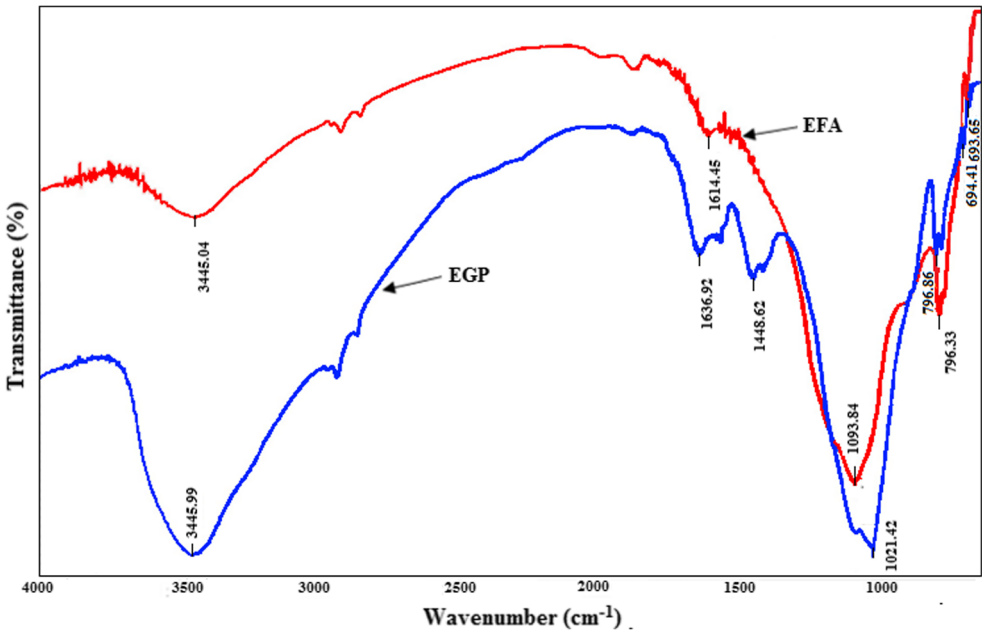

Fig. 2 FTIR spectra of EFA and EGP

The peak signal of EFA is greater than − 108 ppm [40] which is attributed to the formation of Q^4(0Al) unit and belongs to crystalline silica phase. Similarly UFA is also attributed to Q^4(0Al) unit [42] but assigned to the vitreous phase as the peak signal is less than − 108 ppm. The alkali activations of EFA and UFA shifted the peak signals to lower negative values, which indicate the occurrence of chemical reaction and microstructural transformation of Al atoms. The peak signals at -94.6 ppm and − 88.86 ppm of EGP and UGP ascribes to Q^4(2Al) and Q^4(4Al) units respectively [41, 42]. Even though the Al-Si gels are formed in both EGP and UGP, the amount of Al surrounding the Si is higher in UGP when compared to that of EGP. Consequently, a stronger three dimensional Al-Si network is formed in UGP with better interlinked Si-O-Al bonds. Other minor peaks at -87.5 ppm, -102.34 ppm and − 105.92 ppm of EGP indicate the formations of Q^4(4Al), Q^4(1Al) and Q^4(0Al) respectively [42]. The NMR spectra available in the literatures showed intense signals in all the Q^4(mAl) structures (m = 0 to 4) with the assistance of long curing period (24 h) [38, 44]. However, the short curing period (6 h) of the geopolymer paste delays the formation of such pronounced peaks.

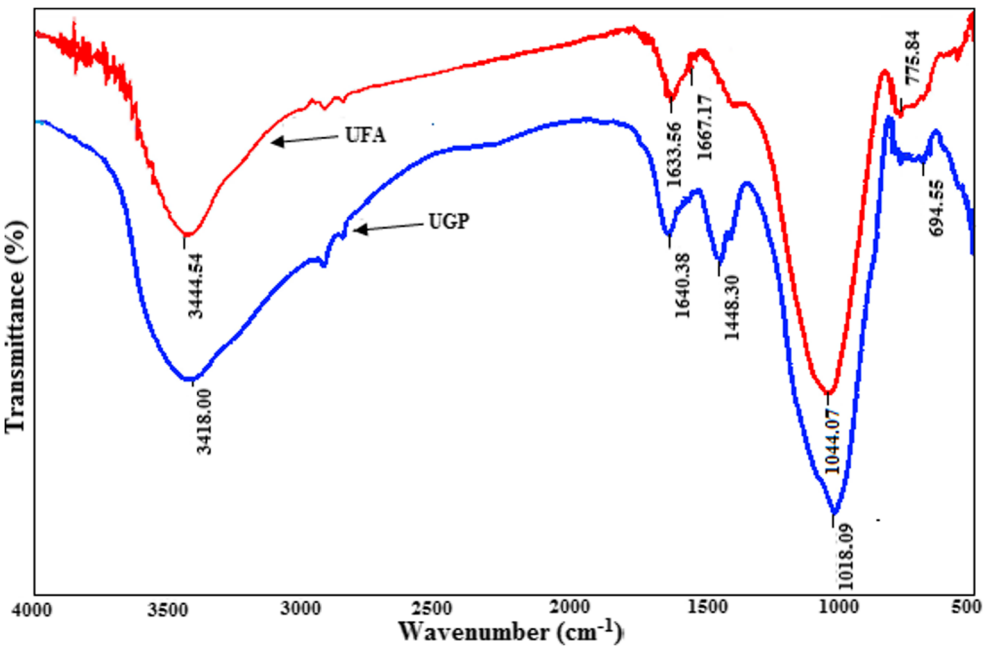

Fig. 3 FTIR spectra of UFA and UGP

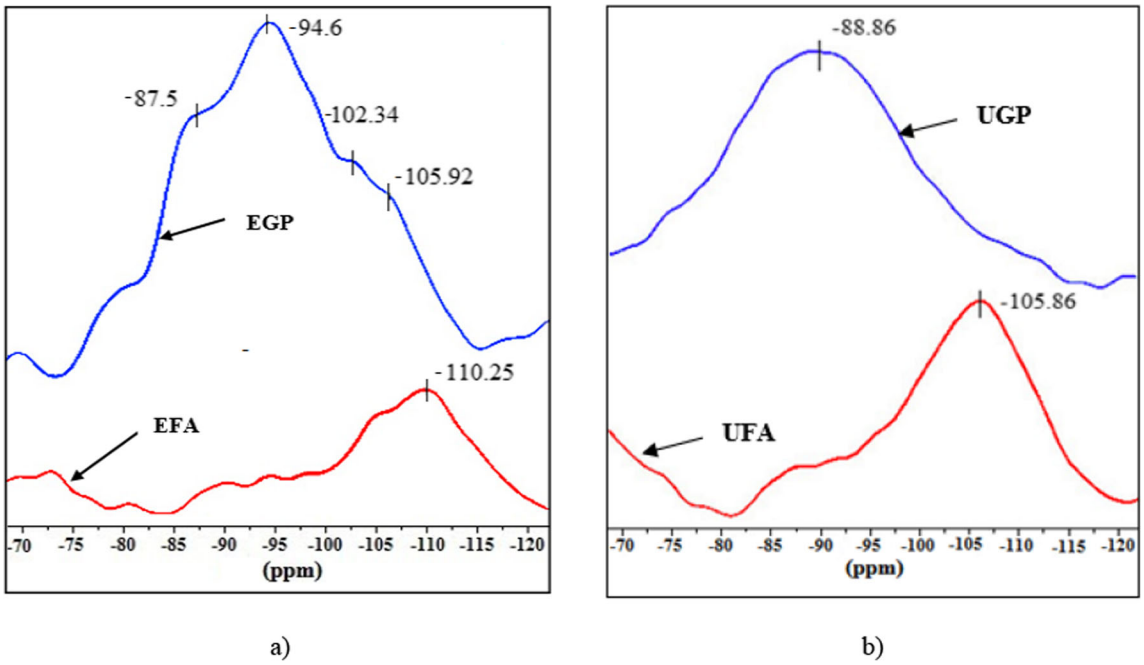

Fig. 4 ^{29}Si MAS NMR spectra **a** EFA and EGP ; **b** UFA and UGP

3.4 Mineralogical Characterization

The X-Ray diffraction (XRD) patterns of the EFA and UFA along with their activated geopolymer pastes are shown in Figs. 5 and 6 respectively. The occurrence of two inherent crystalline phases, namely quartz (PDF# 46-1045) and mullite (PDF#15–776) are identified in EFA with the help of Inorganic Crystal Structure Database (ICSD). The activation of EFA with alkaline solution marginally leached the crystalline quartz (SiO_2) phase with the reduction in the corresponding peak intensities [45, 46]. The long-range orderly crystalline phase of EFA is partially converted into short-range orderly vitreous phase and the hump formation of the regions between 20°2θ and 35°2θ positions [47, 48] indicates the evolution of reactive phase in EGP. It is also seen that the mullite ($3Al_2O_3SiO_2$) phase present in EFA is almost dissolved in EGP due to the establishment of Si-OH and Al-OH monomers. The crystalline phase still exists with some distinguished vitreous phase, irrespective of the occurrence of EFA activation (intrusion of Al to Si).

The UFA and UGP shows vitreous phases in all the position of the XRD patterns. Additionally the vitreous phases are

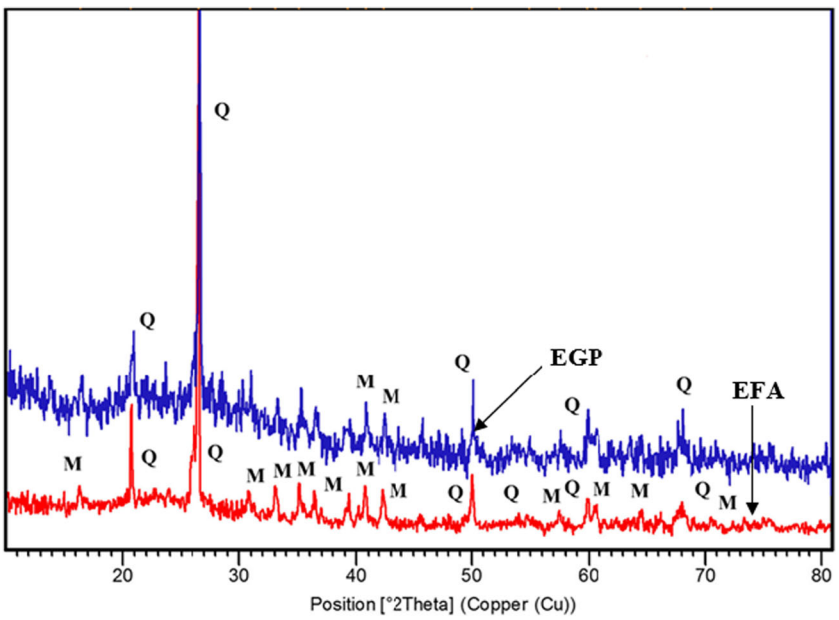

Fig. 5 XRD pattern of EFA and EGP

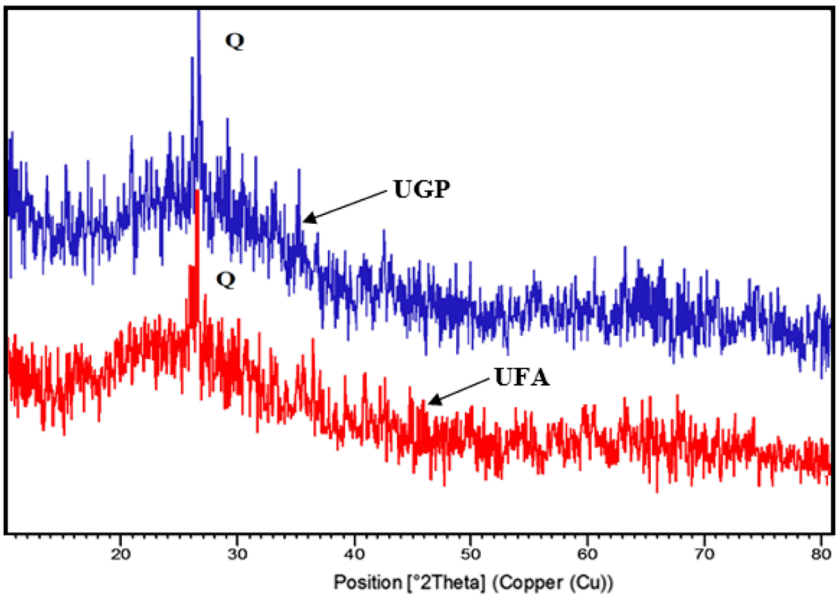

Fig. 6 XRD pattern of UFA and UGP

endorsed by the elevated humps of the regions between 20°2θ and 40°2θ [46, 49]. The only crystalline phase identified in the position of 26.5°2θ is quartz. However, the intensity is reduced in the activated UGP paste due to alkaline solution's leached action. From the literature studies, it is reported that the establishment of the minerals present in the vitreous phase is laborious [47]. The UFA reacts quickly with the alkaline solution due to the presence of vitreous phase. Moreover, the vitreous phase continues to exist in UGP, which indicates further reactive nature of the hardened matrix. As reported in the previous studies, the prolonged curing period (24 h) results in the formation of diverse zeolite species, like hydrated sodalite, Na-chabazite, Zeolite-Y, Zeolite-P, phillipsite, Cancrinite, faujasite-Na and analcime [33, 46, 48, 50]. However, the formations of these zeolite species are not noticed in the present geopolymer XRD patterns due to the short curing time (6 h). Hence results in the formation of metastable/intermediate zeolite precursor [47].

3.5 Microstructure Characterization

The microstructure studies are investigated by using SEM images. The microstructures of EFA and UFA through SEM images are shown in Fig. 7. The UFA particles are generally smooth textured, uniform and spherical as compared to those of EFA particles. Moreover, the EFA particles are larger in size and attached to large number of clustered solids deposits which hinders the dissolution of EFA in alkaline solution as compared to that of UFA.

The microstructures of EGP and UGP by using SEM images are shown in Fig. 8. Significant differences are noticed in the appearances of EGP and UGP solid matrix phases. The surface of EGP is heterogeneous, weakly bonded with few gel matrix accreted the FA remnants and exhibited a frangible structure. Contradictory, the surface of UGP is almost homogenous, densely bonded with interminable matrix phase of reaction products and appeared like a layer of viscous fluid suddenly

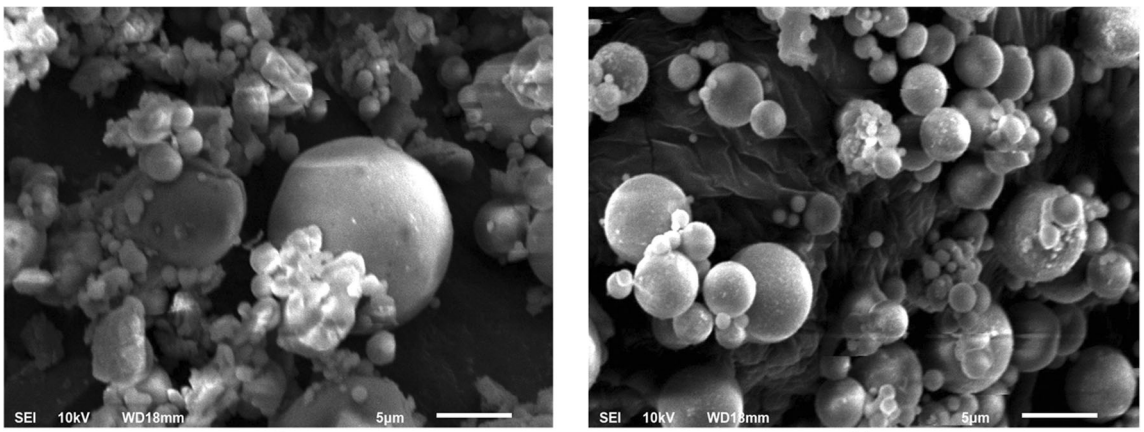

a) b)

Fig. 7 Microstructure of FAs **a** EFA; **b** UFA

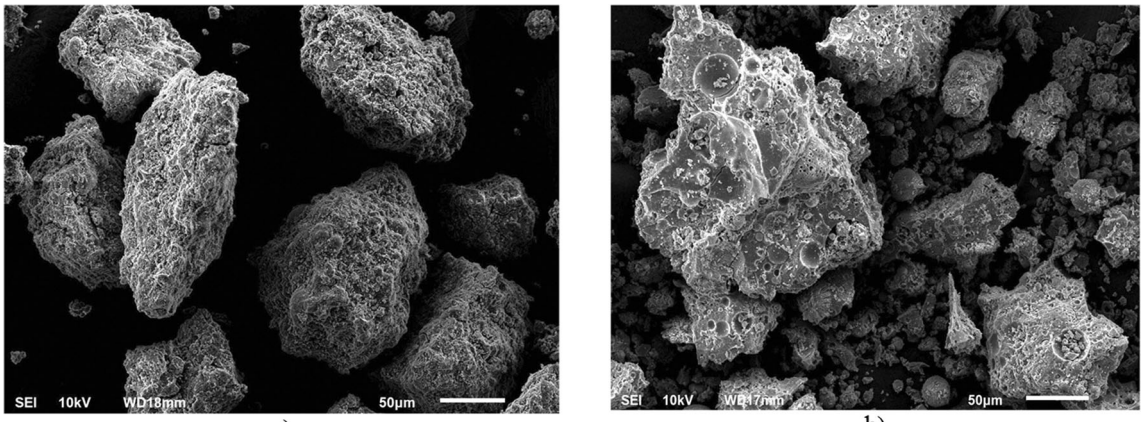

Fig. 8 Microstructure of geopolymer pastes **a** EGP; **b** UGP

frigid [47]. Moreover, the circular cavities that are visible in UGP represent the detachment of the unreacted FA particles.

3.6 Compressive Strength of Geopolymer Concrete

The inferences of characterization of FAs are validated through the assessment of the geopolymer concrete's compressive strength. The variations of the compressive strength for distinct parameters are shown in Fig. 9. It is seen that in the parametric studies, the strength of UGC is superior to that of EGC. Moreover, the variation of the parameters had a negligible effect on the strength of EGC. This remarkable observation justifies the contribution of vitreous Al and Si constituents by the UFA in geopolymer concrete's strength

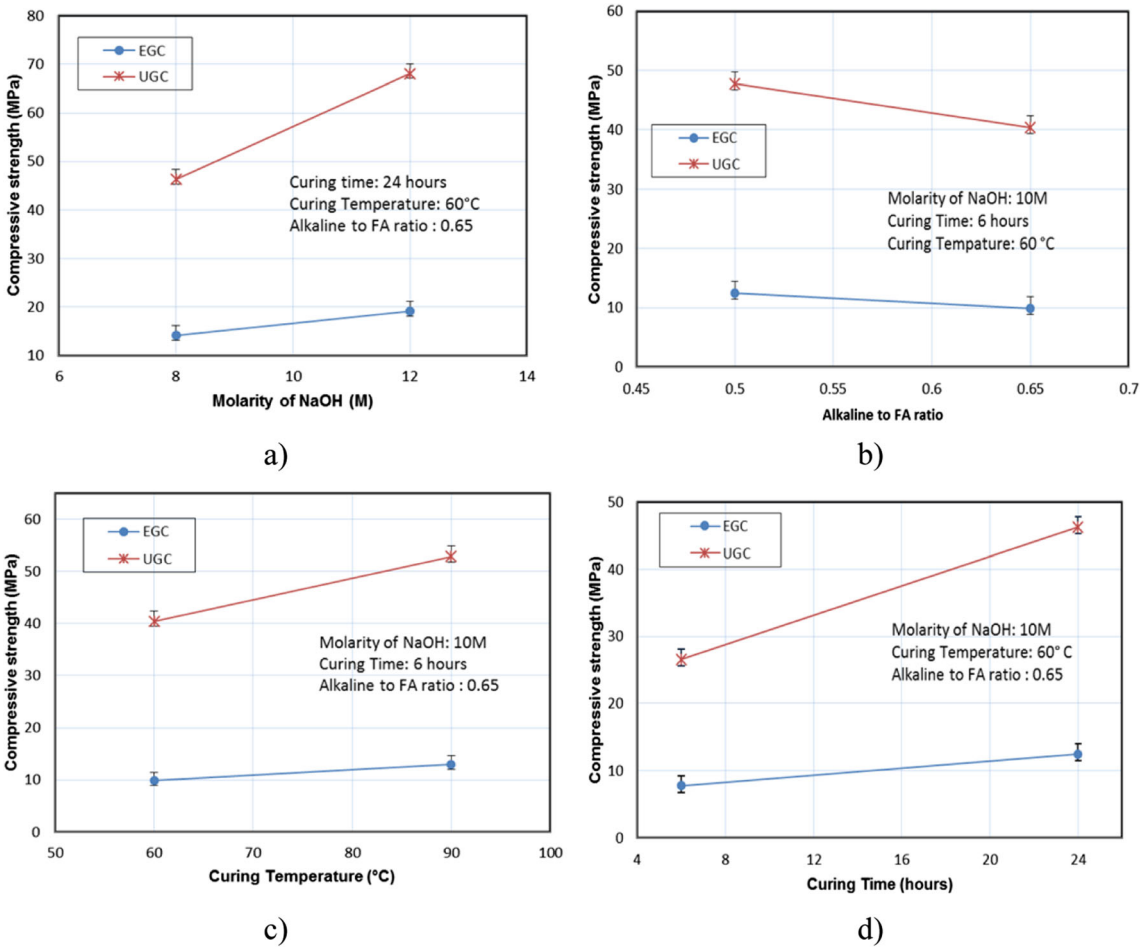

Fig. 9 Variation of compressive strength. **a** Molarity of NaOH; **b** Alkaline to FA ratio; **c** Curing temperature; **d** Curing time

development. The molarity of NaOH and curing condition perform a vital role in the dissolution of Al-Si constituents and polymerization process (strength enhancement), but the role of these parameters effectively dependent on the vitreous Al-Si constituents of FA sources.

4 Conclusions

This paper investigates the suitability of FAs obtained from two different sources for geopolymerisation. The physical, chemical, spectroscopy, mineralogical and microstructural techniques are studied for the characterizations of FAs and associated geopolymer pastes. Moreover, the results are validated with the compressive strength of geopolymers concrete. The subsequent conclusions from the experimental research are drawn:

- Based on the chemical attack, it is found that the quantity of vitreous components (Al & Si) influence the process of geopolymerisation and irrespective of the Al and Si constituents in the FA's chemical composition.
- In contempt to the dissolution and polymerization occurred in EFA, but its crystalline nature yielded in deficient strength development of the activated geopolymer paste which is evident from the FTIR, NMR and XRD characterizations.
- The N-A-S-H gels produced during the geopolymeriation of EFA and UFA were the zeolite precursors (metastable/ intermediate phase) and vitreous in short range owing to the short (6 h) curing period.
- The strength of geopolymer concrete purely depends on the fineness of particle size and the presence of the vitreous Al and Si constituents in the FA.
- The rate of strength enhancement in EGC is less dependent on the variation of typical parameters such as NaOH molarity, alkaline to FA ratio, curing temperature and curing time. The reasons are less amount of vitreous Al and Si constituents and larger particle size as compared to those of UGC.

Based on the characterization techniques, the reactive nature of UFA is superior to that of EFA. Thus, the characterization of FA sources by different techniques is required for the identification of its potential reactivity prior to the synthesis of geopolymers and to adopt this technology in the construction sector. In that way, the extreme variation of the geopolymer synthesis parameters leading to undesirable production cost and hazardous work environment can be avoided.

Acknowledgements The authors whole-heartily wish to acknowledge the financial support provided by the University Grants Commission, India.

Author Contributions Thulasirajan Krishnan: Conceptualization, Methodology, Formal analysis and investigation, Writing - original draft preparation and Writing - editing.

Revathi Purushothaman: Supervision, Funding acquisition and Writing - review.

Funding This work was funded by University Grants Commission (UGC), India through Major Research Project Scheme. (Grant no: F. No-43-259/2014(SR) and 28.07.2015)

Data Availability All the data are available in the form of figures and tables.

Code Availability Not applicable.

Declarations This manuscript has been published elsewhere in any form or language and has not been submitted to more than one journal for simultaneous consideration.

Conflicts of Interest/Competing Interests The authors have no conflicts of interest to declare that are relevant to the content of this article.

Consent to Participate Not applicable.

Consent for Publication Not applicable.

References

1. Central Electricity Authority (2020) Report on fly ash generation at coal/lignite based Thermal Power Stations and its utilization in the country for the year 2018-19, Minister of Power, New Delhi, India January, 2020. https://cea.nic.in/reports/others/thermal/ tcd/flyash_201819.pdf. Accessed 04.11.2020
2. Palomo A, Grutzeck MW, Blanco MT (1999) Alkali-activated fly ashes: A cement for the future. Cem Concr Res 29:1323–1329. https://doi.org/10.1016/S0008-8846(98)00243-9
3. Fernandez-Jimenez A, Palomo A (2005) Mid-infrared spectroscopic studies of alkali-activated fly ash structure. Micropor Mesopor Mat 86:207–214. https://doi.org/10.1016/j.micromeso.2005.05.057
4. Chithambaram SJ, Kumar S, Prasad MM, Adak D (2018) Effect of parameters on the compressive strength of fly ash based geopolymer concrete. Struct Concr 19:1202–1209. https://doi.org/10.1002/suco.201700235
5. Joseph B, Mathew G (2012) Influence of aggregate content on the behavior of fly ash based geopolymer concrete. Sci Iran 19:1188–1194. https://doi.org/10.1016/j.scient.2012.07.006
6. Vora PR, Dave UV (2013) Parametric studies on compressive strength of geopolymer concrete. Procedia Eng 51:210–219. https://doi.org/10.1016/j.proeng.2013.01.030
7. Somna K, Jaturapitakkul C, Kajitvichyanukul P, Chindaprasirt P (2011) NaOH-activated ground fly ash geopolymer cured at ambient temperature. Fuel 90:2118–2124. https://doi.org/10.1016/j.fuel.2011.01.018
8. Ahmed MF, Nuruddin MF, Nasir Shafiq N (2011) Compressive strength and workability characteristics of low-calcium fly ash-based self compacting geopolymer concrete. Int J Arch Civ Constr Sci Environ Eng. https://doi.org/10.5281/zenodo.1330481
9. Nath P, Sarker PK (2015) Use of OPC to improve setting and early strength properties of low calcium fly ash geopolymer concrete cured at room temperature. Cem Concr Compos 55:205–214. https://doi.org/10.1016/j.cemconcomp.2014.08.008

10. Hardjito D, Rangan BV (2005) Development and properties of low calcium fly ash based geopolymer concrete. Curtin University of Technology, Perth. http://hdl.handle.net/20.500.11937/5594. Accessed 04.11.2020
11. Gunasekara C, Law DW, Setunge S (2016) Long term engineering properties of fly ash geopolymer concrete. SCMT4 LasVegas, USA. http://www.claisse.info/2016%20papers/S109.pdf. Accessed 04.11.2020
12. Hardjito D, Wallah SE, Sumajouw DMJ, Rangan BV (2004) On the development of fly ash-based geopolymer concrete. Mater J 101: 467–472
13. Olivia M, Nikraz H (2012) Properties of fly ash geopolymer concrete designed by taguchi method. Mater Des 36:191–198. https://doi.org/10.1016/j.matdes.2011.10.036
14. Sumajouw DMJ, Hardjito D, Wallah SE, Rangan BV (2007) Fly ash-based geopolymer concrete: study of slender reinforced columns. J Mater Sci 42:3124–3130. https://doi.org/10.1007/s10853-006-0523-8
15. Krishnan T, Purushothaman R (2017) Effect of molarity of sodium hydroxide and curing temperature on the strength of geopolymer concrete containing recycled concrete aggregate. In: Proceeding of the International Conference on Advances in Construction Materials and Systems (ICACMS) 4:45–53
16. Junaid MT, Kayali O, Khennane A, Black J (2015) A mix design procedure for low calcium alkali activated fly ash-based concretes. Construct Build Mater 79:301–310
17. Bakharev T (2005) Geopolymeric materials prepared using class F fly ash and elevated temperature curing. Cem Concr Res 35:1224–1232. https://doi.org/10.1016/j.cemconres.2004.06.031
18. Criado M, Palomo A, Fernandez-Jimenez A (2005) Alkali activation of fly ashes. Part 1: Effect of curing conditions on the carbonation of the reaction products. Fuel 84:2048–2054. https://doi.org/10.1016/j.fuel.2005.03.030
19. Rickard WDA, Williams R, Temuujin J, Riessen AV (2011) Assessing the suitability of three Australian fly ashes as an aluminosilicate source for geopolymers in high temperature applications. Mater Sci Eng A 528:3390–3397. https://doi.org/10.1016/j.msea.2011.01.005
20. Temuujin J, Rickard W, Riessen AV (2013) Characterization of various fly ashes for preparation of geopolymers with advanced applications. Adv Powder Technol 24:495–498. https://doi.org/10.1016/j.apt.2013.01.013
21. Williams RP, Riessen AV (2010) Determination of the reactive component of fly ashes for geopolymer production using XRF and XRD. Fuel 89:3683–3692. https://doi.org/10.1016/j.fuel.2010.07.031
22. Valcke SLA, Pipilikaki P, Fischer HR, Verkuijlen MHW, Eck ERHV (2015) FT-IR and ^{29}Si-NMR for evaluating aluminium–silicate precursors for geopolymers. Mater Struct 48:557–569. https://doi.org/10.1617/s11527-014-0432-2
23. Nikolic V, Komljenovic M, Bascarevic Z, Marjanovic N, Miladinovic Z, Petrovic R (2015) The influence of fly ash characteristics and reaction conditions on strength and structure of geopolymers. Constr Build Mater 94:361–370. https://doi.org/10.1016/j.conbuildmat.2015.07.014
24. Korniejenko K, Łach M, Marczyk J, Ziejewska C, Halyag NP, Mucsi G (2019) Fly ash as a raw material for geopolymerisation-mineralogical composition and morphology. IOP Conf Seri: Mater Sci Eng 706:012006. https://doi.org/10.1088/1757-899X/706/1/012006
25. Korniejenko K, Halyag NP, Mucsi G (2019) Fly ash as a raw material for geopolymerisation - chemical composition and physical properties. IOP Conf Seri: Mater Sci Eng 706:012002. https://doi.org/10.1088/1757-899X/706/1/012002
26. Hadi MNS, Al-Azzawi M, Yu T (2018) Effects of fly ash characteristics and alkaline activator components on compressive strength of fly ash-based geopolymer mortar. Constr Build Mater 175:41–54. https://doi.org/10.1016/j.conbuildmat.2018.04.092
27. Kumar S, Mucsi G, Kristály F, Pekker P (2017) Mechanical activation of fly ash and its influence on micro and nano-structural behaviour of resulting geopolymers. Adv Powder Technol 28: 805–813. https://doi.org/10.1016/j.apt.2016.11.027
28. Wang T, Ishida T, Gu R (2020) A study of the influence of crystal component on the reactivity of low-calcium fly ash in alkaline conditions based on SEM-EDS. Constr Build Mater 243:1–14. https://doi.org/10.1016/j.conbuildmat.2020.118227
29. Risdanareni P, Puspitasari P, Jaya EJ (2017) Chemical and physical characterization of fly ash as geopolymer material. MATEC Web Conf 97:01031. https://doi.org/10.1051/matecconf/20179701031
30. Diaz EI, Allouche EN, Eklund S (2010) Factors affecting the suitability of fly ash as source material for geopolymers. Fuel 89:992–996. https://doi.org/10.1016/j.fuel.2009.09.012
31. Assi LN, Carter K, Deaver E, Ziehl P (2020) Review of availability of source materials for geopolymer/sustainable concrete. J Clean Prod 263:1–13.https://doi.org/10.1016/j.jclepro.2020.121477
32. Fernandez-Jimenez A, Torre AGDL, Palomo A, López-Olmo G, Alonso MM, Aranda MAG (2006) Quantitative determination of phases in the alkali activation of fly ash. Part II: Degree of reaction. Fuel 85:1960–1969. https://doi.org/10.1016/j.fuel.2006.04.006
33. Criado M, Fernandez-Jimenez A, Torre AGDL, Aranda MAG, Palomo A (2007) An XRD study of the effect of the SiO_2/Na_2O ratio on the alkali activation of fly ash. Cem Concr Res 37:671–679. https://doi.org/10.1016/j.cemconres.2007.01.013
34. Komljenovi M, Bacarevic Z, Bradic V (2010) Mechanical and microstructural properties of alkali-activated fly ash geopolymers. J Hazard Mater 181:35–42. https://doi.org/10.1016/j.jhazmat.2010.04.064
35. ASTM C618-12a (2012) Standard specification for coal fly ash and raw or calcined natural pozzolan for use in concrete. ASTM International, West Conshohocken. www.astm.org
36. Palomo A, Alonso S, Fernandez-Jimenez A, Sobrados I, Sanz J (2004) Alkaline activation of fly ashes: NMR study of the reaction products. J Am Ceram Soc 87:1141–1145. https://doi.org/10.1111/j.1551-2916.2004.01141.x
37. Palomo A, Fernndez-Jimenez A, Criado M (2004) Geopolymers: same basic chemistry, different microstructures. Mater Constr 54: 77–91
38. Criado M, Fernandez Jimenez A, Sobrados I, Palomo A, Sanz J (2012) Effect of relative humidity on the reaction products of alkali activated fly ash. J Eur Ceram Soc 32:2799–2807. https://doi.org/10.1016/j.jeurceramsoc.2011.11.036
39. Guo X, Shi H, Dick WA (2010) Compressive strength and microstructural characteristics of class C fly ash geopolymer. Cem Concr Compos 32:142–147. https://doi.org/10.1016/j.cemconcomp.2009.11.003
40. Barbosa VFF, MacKenzie KJD, Thaumaturgo C (2000) Synthesis and characterisation of materials based on inorganic polymers of alumina and silica: sodium polysialate polymers. Int J Inorg Mater 2:309–317. https://doi.org/10.1016/S1466-6049(00)00041-6
41. Engelhardt G, Lippmaa E, Magi M (1981) Ordering of silicon and aluminum ions in the framework of NaX zeolites - A solid-state high-resolution ^{29}Si n.m.r. study. J Chem Soc Chem Commun 14: 712–713
42. Davidovits J (2015) Geopolymer chemistry and applications, 4th edn. Geopolymer Institute, Saint- Quentin
43. Engelhardth G, Michel D (1987) High resolution solid state NMR of silicates and zeolites. Wiley, New York
44. Fernandez-Jimenez A, Palomo A, Sobrados I, Sanz J (2006) The role played by the reactive alumina content in the alkaline activation of fly ashes. Micropor Mesopor mater 91:111–119. https://doi.org/10.1016/j.micromeso.2005.11.015

45. Alvarez-Ayuso E, Querol X, Plana F et al (2008) Environmental, physical and structural characterisation of geopolymer matrixes synthesised from coal (co-)combustion fly ashes. J Hazard Mater 154:175–183. https://doi.org/10.1016/j.jhazmat.2007.10.008
46. Fernandez-Jimenez A, Palomo A (2005) Composition and microstructure of alkali activated fly ash binder: Effect of the activator. Cem Concr Res 35:1984–1992. https://doi.org/10.1016/j.cemconres.2005.03.003
47. Ryu GS, Lee YB, Koh KT, Chung YS (2013) The mechanical properties of fly ash-based geopolymer concrete with alkaline activators. Constr Build Mater 47(2013):409–418. https://doi.org/10.1016/j.conbuildmat.2013.05.069
48. Criado M, Fernandez-Jimenez A, Palomo A, Sobrados I, Sanz J (2008) Effect of the SiO_2/Na_2O ratio on the alkali activation of fly ash. Part II: ^{29}Si MAS-NMR Survey. Micropor Mesopor Mat 109:525–534. https://doi.org/10.1016/j.micromeso.2007.05.062
49. Marjanovic N, Komljenovic M, Bascarevic Z, Nikolic V (2014) Improving reactivity of fly ash and properties of ensuing geopolymers through mechanical activation. Construct Build Mater 57:151–162. https://doi.org/10.1016/j.conbuildmat.2014.01.095
50. Hajimohammadi A, Provis JL, Van Deventer JSJ (2011) The effect of silica availability on the mechanism of geopolymerisation. Cem Concr Res 41:210–216. https://doi.org/10.1016/j.cemconres.2011.02.001